In Situ Supramolecular Assembly and Modular Modification of Hyaluronic Acid Hydrogels for 3D Cellular Engineering

9 AUTHORS, INCLUDING:

Kyeng Min Park
Institute for Basic Science
24 PUBLICATIONS **1,169** CITATIONS

SEE PROFILE

Junseok Yeom
LG Household and Healthcare
20 PUBLICATIONS **263** CITATIONS

SEE PROFILE

Kimoon Kim
Pohang University of Science and Technology
298 PUBLICATIONS **19,318** CITATIONS

SEE PROFILE

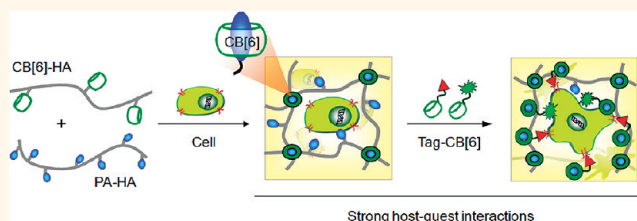# *In Situ* Supramolecular Assembly and Modular Modification of Hyaluronic Acid Hydrogels for 3D Cellular Engineering

Kyeng Min Park,[†,¶] Jeong-A Yang,[‡,¶] Hyuntae Jung,[§] Junseok Yeom,[‡] Ji Sun Park,[⊥] Keun-Hong Park,[⊥] Allan S. Hoffman,[∥] Sei Kwang Hahn,[‡,§,*] and Kimoon Kim[†,§,*]

[†]Center for Smart Supramolecules, Department of Chemistry, Division of Advanced Materials Science, [‡]Department of Materials Science and Engineering, and [§]School of Interdisciplinary Bioscience and Bioengineering, Pohang University of Science and Technology (POSTECH), San 31, Hyoja-dong, Nam-gu, Pohang, Kyungbuk 790-784, Korea, [⊥]Department of Biomedical Science, College of Life Science, CHA University, 606-16, Yeoksam 1-dong, Kangnam-gu, Seoul, 135-081, Korea, and [∥]Department of Bioengineering, University of Washington, Box 351720, Seattle, Washington 98195, United States. [¶]These authors contributed equally to this work.

Extracellular matrix (ECM) plays a crucial role in defining the 3D environment of cells.[1] Recently, synthetic hydrogels have emerged as highly promising scaffolds to reconstitute artificial 3D environments that mimic the ECM for both *in vitro* and *in vivo* tissue engineering applications.[2−4] A crucial challenge for such hydrogels is the facile formation and modular modification of the hydrogels in the presence of cells to ensure that cells are exposed to the proper cues for cellular proliferation and differentiation at the right place and time. Strategies for the hydrogel formation and modification generally require highly reactive chemicals, noncovalent interactions such as ionic interactions and hydrogen bonding,[5−7] and/or external stimuli such as light[8] and temperature[9] or pH change.[10] However, most of these interactions are, up to date, neither controllable nor sufficiently stable in the body, causing a significant cytotoxicity in some cases.[11]

On the other hand, supramolecular hydrogels have been developed using natural host−guest (receptor−ligand) pairs[12,13] like (strep)-avidin−biotin [(S)Av-Bt] with an extremely high binding affinity ($K \sim 10^{13}−10^{15}$ M^{-1}), but their efficient exploitation has been hampered by the difficulties in chemical modification and mass production as well as the unknown immunogenicity of (S)Av. Alternatively, hydrogels based on synthetic host−guest pairs, such as α-cyclodextrin-polyethyleneglycol (α-CD-PEG)[14−16] and β-CD-adamantane (β-CD-Ad),[17] have been developed, which have an intrinsic limitation for *in vivo* applications due to the low binding affinity of CDs to their guests (α-CD-PEG, $K \sim 10^2$ M^{-1}, and β-CD-Ad, $K \sim 10^5$ M^{-1}). Cucurbit[6]uril (CB[6]), a member of the

hollowed-out-pumpkin-shaped host family, cucurbit[*n*]uril (*n* = 5−8, 10; CB[*n*]), has exceptionally high binding affinity and selectivity toward alkylammonium ions in aqueous solution.[18,19] In particular, it tightly binds polyamines (PA) like 1,6-diaminohexane (DAH) or spermine (SPM) (in their protonated forms) to make ultrastable 1:1 host−guest complexes with a binding constant up to 10^{10} or 10^{12} M^{-1}, which is almost comparable to that of streptavidin and

ABSTRACT

A facile *in situ* supramolecular assembly and modular modification of biocompatible hydrogels were demonstrated using cucurbit[6]uril-conjugated hyaluronic acid (CB[6]-HA), diaminohexane-conjugated HA (DAH-HA), and tags-CB[6] for cellular engineering applications. The strong and selective host−guest interaction between CB[6] and DAH made possible the supramolecular assembly of CB[6]/DAH-HA hydrogels in the presence of cells. Then, the 3D environment of CB[6]/DAH-HA hydrogels was modularly modified by the simple treatment with various multifunctional tags-CB[6]. Furthermore, we could confirm *in situ* formation of CB[6]/DAH-HA hydrogels under the skin of nude mice by sequential subcutaneous injections of CB[6]-HA and DAH-HA solutions. The fluorescence of modularly modified fluorescein isothiocyanate (FITC)-CB[6] in the hydrogels was maintained for up to 11 days, reflecting the feasibility to deliver the proper cues for cellular proliferation and differentiation in the body. Taken together, CB[6]/DAH-HA hydrogels might be successfully exploited as a 3D artificial extracellular matrix for various tissue engineering applications.

KEYWORDS: cucurbituril · hyaluronic acid · hydrogels · supramolecular chemistry · tissue engineering
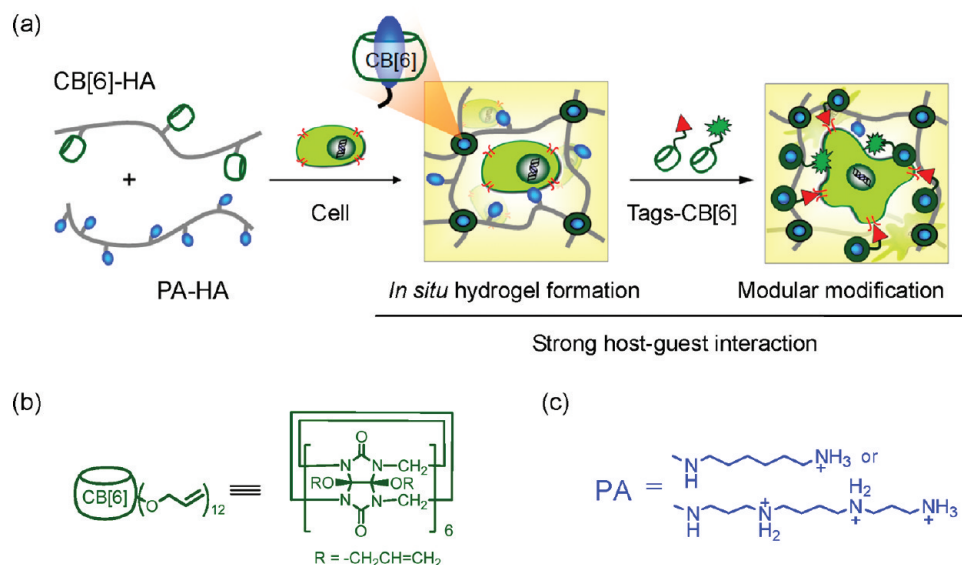
Figure 1. (a) Schematic representations for *in situ* formation of supramolecular biocompatible hydrogel and its modular modification using highly selective and strong host–guest interactions. The simple mixing of cucurbit[6]uril-conjugated hyaluronic acid (CB[6]-HA) and polyamine-conjugated HA (PA-HA) resulted in the formation of CB[6]/PA-HA hydrogel, which was further modularly modified with various tags-CB[6]. The chemical structures of (b) CB[6] and (c) PAs of diaminohexane (DAH) and spermine (SPM).

biotin (SAv-Bt, $K \sim 10^{13}$ M^{-1}).[20] The exceptional selectivity and stability under physiological conditions, as well as negligible cytotoxicity, make CB-PA pairs a useful tool for the noncovalent conjugation and modification of CB-based nanomaterials.[21−23]

In this work, we report a facile supramolecular strategy for the formation of biocompatible hyaluronic acid (HA) hydrogels in the presence of cells taking advantage of the highly selective and strong host–guest interaction of CB[6]-PA as a driving force for the cross-linking of biopolymer chains. As shown in Figure 1, our approach involves (1) conjugation of a CB[6] derivative to HA for the synthesis of a host-attached HA (CB[6]-HA) and attachment of PA such as DAH or SPM to HA for the preparation of a guest-attached HA (DAH-HA or SPM-HA), (2) simple mixing of CB[6]-HA with either DAH-HA or SPM-HA to produce a hydrogel *in situ* in the presence of cells without additional reagents and stimuli, and (3) further modular modification of the hydrogel with various "tags"-attached CB[6] (tags-CB[6]), which can be anchored at the residual DAH moieties on the hydrogel by host–guest chemistry. HA is a naturally occurring linear polysaccharide in the body and one of main components of ECM.[24] The CB[6]/PA-HA hydrogels with a good mechanical stability, enzymatic degradability, and negligible toxicity are assessed *in vitro* and *in vivo* and discussed for various biomedical applications such as 3D cell culture, cell therapy, and tissue engineering.

RESULTS AND DISCUSSION

Preparation and Characterization of CB[6]/PA-HA Hydrogels. CB[6]-HA was synthesized by thiol–ene "click" reaction[25] of HS-HA[26] with (allyloxy)$_{12}$CB[6] as we previously reported elsewhere.[27,28] The successful conjugation of (allyloxy)$_{12}$CB[6] to HS-HA was confirmed by FT-IR and ^{1}H NMR analyses.[28] The integral ratio on the ^{1}H NMR spectrum suggested that 6 ± 1 mol % of HA units on average was modified with (allyloxy)$_{12}$CB[6]. DAH-HA and SPM-HA were also synthesized as a counterpart to CB[6]-HA for the hydrogel formation.[26] Approximately 50 ± 2 and 52 ± 2 mol % of HA units on average were modified with DAH and SPM, respectively (Figure 2a and Figure S1a in Supporting Information). The complex formation of DAH or SPM moieties on HA with CB[6] was evidenced by the peak shift from 1.4−1.8 to 0.3−1.0 ppm for DAH or from 1.7 to 0.5 ppm for SPM and the new peak appearance at 4.3, 5.5, and 5.8 ppm for the aliphatic protons of the alkylammonium units in the cavity of CB[6] on the ^{1}H NMR spectra (Figures 2b and S1b). The simple mixing of equal volumes of CB[6]-HA (300 μL, 2.0 wt %) and DAH-HA (300 μL, 2.0 wt %) solutions for 10 s produced a CB[6]/DAH-HA hydrogel (see movie S1 in Supporting Information). The formation of CB[6]/DAH-HA hydrogel was also monitored by dynamic time sweep rheological analysis (Figure 3a). The gelation point at which G′ (storage modulus) and G″ (loss modulus) cross was observed within 2 min at a constant frequency of 100 rad/s. The storage modulus of the CB[6]/DAH-HA hydrogel (1.0 cm in diameter and 0.3 mm in thickness) was measured to be 2.4 ± 0.2 kPa by the frequency sweep rheological analysis (Figure 3b). The CB[6]/DAH-HA hydrogel was soft but robust enough to hold its shape in a centimeter scale (Figure S2). The addition of excess SPM to the hydrogel resulted in a phase transition from gel to sol within 10 min (Figure 3c), and no gelation occurred when CB[6]-HA was added to DAH-HA in the presence of
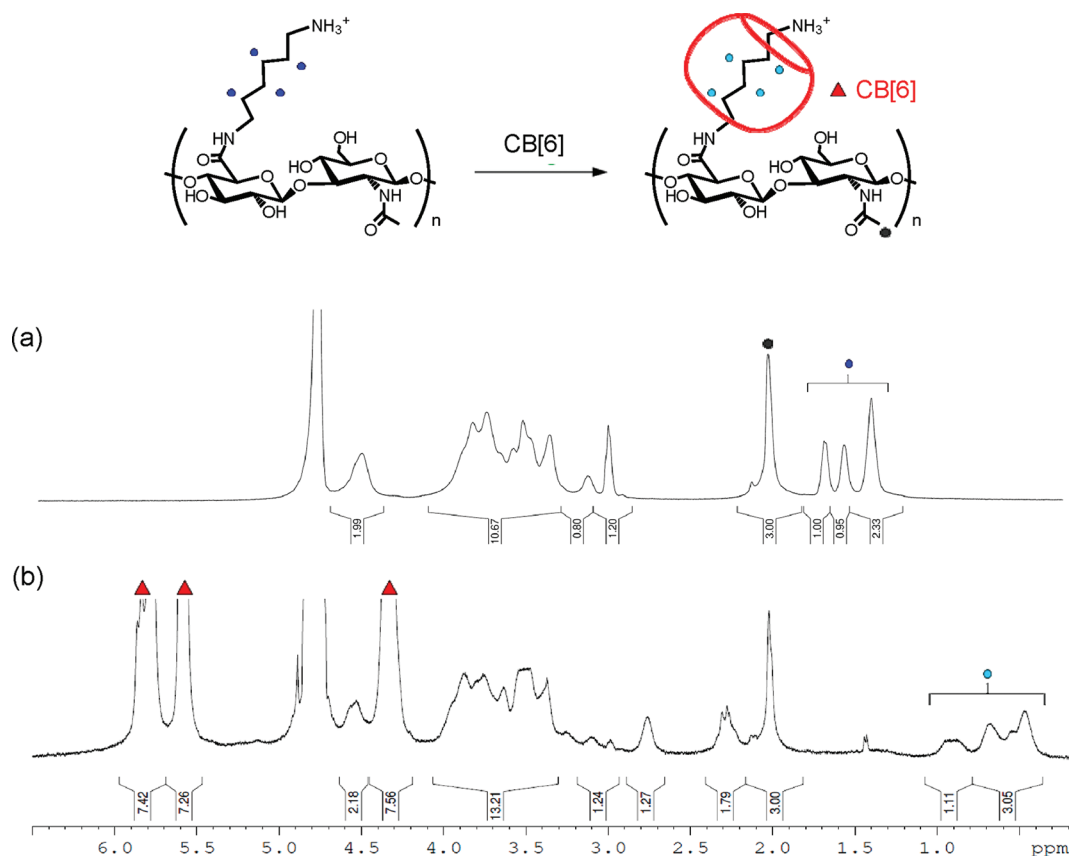
Figure 2. Schematic representation for the host—guest interaction of DAH-HA with CB[6]. ^{1}H NMR spectra of (a) DAH-HA (50 ± 2 mol % of DAH on HA units) and (b) DAH-HA modularly modified with CB[6] by simple mixing in aqueous solution.
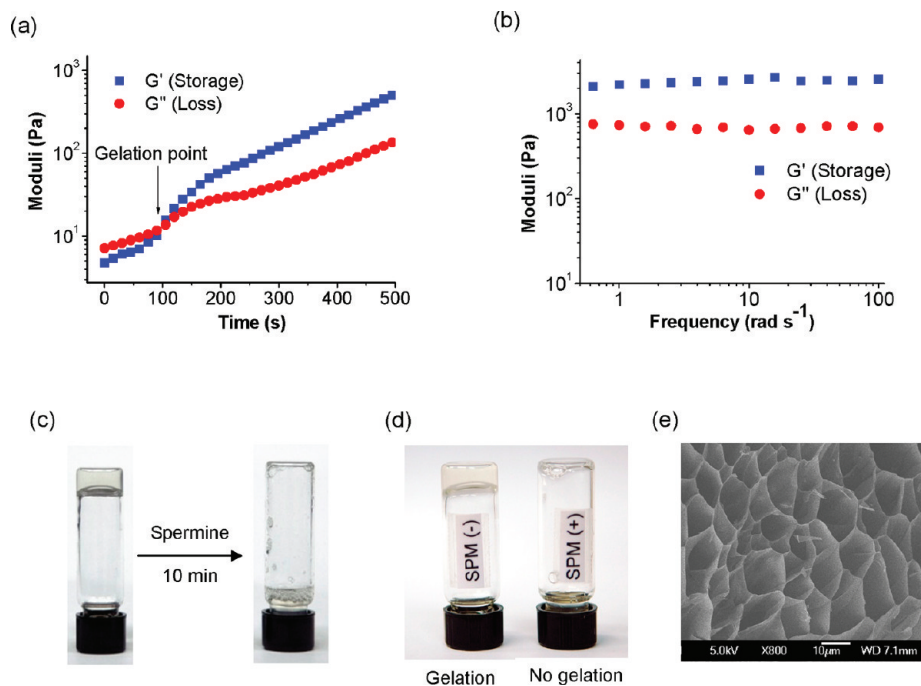
Figure 3. (a) Time sweep rheological analysis at a constant frequency of 100 rad/s. (b) Frequency sweep rheological analysis for storage (G′) and loss (G″) moduli of CB[6]/DAH-HA hydrogel. (c) Phase transition from gel to sol upon addition of excess amount of SPM to CB[6]/PA-HA hydrogel. (d) Inhibition of the CB[6]/DAH-HA hydrogel formation by the addition of excess amount of SPM (1.0 mg) to CB[6]-HA solution (300 μL, 2.0 wt %) before mixing with DAH-HA solution (300 μL, 2.0 wt %). (e) SEM of CB[6]/DAH-HA hydrogel coated with Pt (scale bar = 10 μm).

(a)

(b)

(c)

Figure 4. NIH3T3 cells in (a) CB[6]/DAH-HA hydrogels and (b) CB[6]/SPM-HA hydrogels stained with calcein AM (live cells, green) and EthD-1 (dead cells, red) after incubation at 5% CO_2 and 37 °C for 3 days (scale bar = 50 μm). (c) Quantitative analysis for the number of live and dead cells in 500 μm × 500 μm on the images (mean ± SD, n = 4).
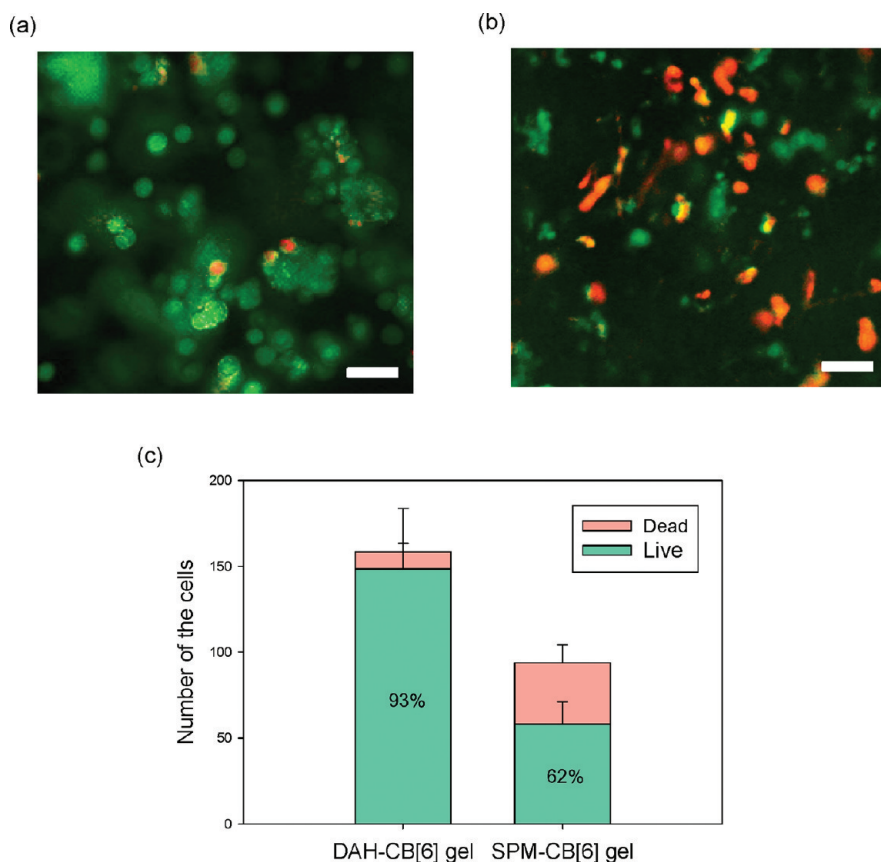
excess SPM (Figure 3d). The results suggested that the host–guest interaction between CB[6] and DAH was responsible for the hydrogel formation. Figure 3e shows the porous microstructure of the CB[6]/DAH-HA hydrogel by scanning electron microscopy (SEM). Similar with DAH-HA, SPM-HA also formed a CB[6]/SPM-HA hydrogel upon mixing with CB[6]-HA. Its storage modulus was measured to be 3.4 ± 0.5 kPa, 1.4-fold higher than that of the CB[6]/DAH-HA hydrogel (Figure S3a), which could be ascribed to the stronger host–guest interaction between SPM and CB[6] than that between DAH and CB[6]. From the results, it was thought that a diverse array of hydrogels with different physical and mechanical properties might be prepared by altering the binding affinity of guest molecules.

Cytocompatibility of CB[6]/DAH-HA Hydrogels. To test *in situ* formation of CB[6]/DAH-HA hydrogels in the presence of cells, DAH-HA (10.0 μL, 2.0 wt %) and CB[6]-HA (10 μL, 2.0 wt %) solutions were mixed with NIH3T3 cells, which readily resulted in the formation of a cell-entrapped hydrogel. The cytotoxicity of the hydrogel to NIH3T3 cells was assessed using the standard live/dead cell assay with calcein AM and EthD-1 to stain live cells in green and dead cells in red, respectively. More than *ca.* 93% of the cells in CB[6]/DAH-HA hydrogels appeared to be alive, emitting green fluorescence even

after incubation for 3 days (Figure 4a,c), whereas the cell viability was lower than *ca.* 62% with a smaller number of the cells for the case of CB[6]/SPM-HA hydrogels (Figure 4b,c). Since biodegradability is another important property for 3D artificial ECM,[3,29] the enzymatic degradation of the cell-containing CB[6]/DAH-HA hydrogel was examined after treatment with hyaluronidase (HAase), an endoglycosidic enzyme produced by cells to remodel ECM for proliferation and migration in tissues.[30] The hydrogel degraded almost completely in 24 h to release the cells at the bottom of a well plate where they continued to proliferate as observed by optical microscopy (Figure 5). The *in situ* formation of hydrogels in the presence of cells with a high cell viability, enzymatic degradability, and negligible cytotoxicity is the unique characteristics of CB[6]/DAH-HA hydrogels for the applications to 3D cellular engineering.

Modular Modification of CB[6]/DAH-HA Hydrogels with Tags-CB[6]. Another unique feature of the supramolecular hydrogel is its facile, noncovalent, and modular modification. Within the CB[6]/DAH-HA hydrogels prepared with an equal volume of CB[6]-HA (CB[6] content of 6 ± 1 mol %) and DAH-HA (DAH content of 50 ± 2 mol %) solutions (2 wt % each), a majority of the DAH moieties remain uncomplexed, which can further interact with
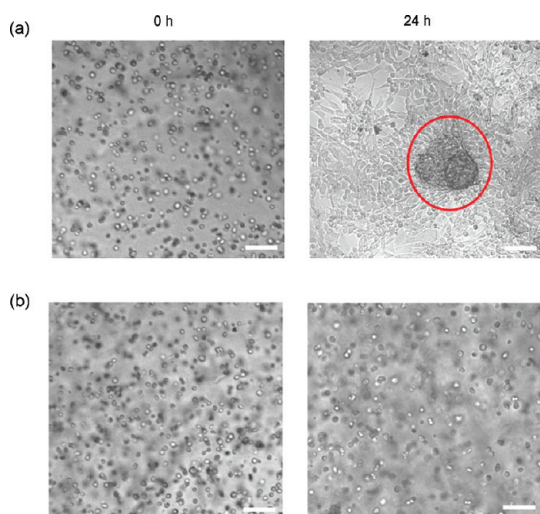
Figure 5. Optical microscopic images of cell-entrapped CB[6]/DAH-HA hydrogels after treatment (a) with and (b) without hyaluronidase (scale bar = 100 μm). The red circle indicates partial remnants of the CB[6]/DAH-HA hydrogel after enzymatic degradation with hyaluronidase for 24 h.

additional CB[6] derivatives. Accordingly, we could easily modify CB[6]/DAH-HA hydrogels with various functional tags-CB[6], including fluorescent-dye-conjugated CB[6] such as fluorescein isothiocyanate (FITC)-CB[6] and rhodamine B isothiocyanate (RBITC)-CB[6] (Figure S4) during and even after the hydrogel formation. CB[6]/DAH-HA hydrogels treated with a solution of RBITC-CB[6] (up to 0.1 equiv to DAH moiety on DAH-HA) maintained fluorescence after washing for a day (Figures 6a and S2b). Furthermore, the RBITC-CB[6]@CB[6]/DAH-HA hydrogel retained *ca.* 60% of the initial fluorescence intensity for up to 420 h in PBS (Figure 6d), reflecting the stability of host−guest interaction between the tag-CB[6] and the DAH moiety on the hydrogel. In contrast, CB[6]/DAH-HA hydrogel treated with simple RhoB (the unconjugated fluorophore of RBITC) instead of RBITC-CB[6] showed a rapid decrease in fluorescence intensity (less than 5% of the initial intensity) within 3 h (Figure 6c,d). Interestingly, green and red fluorescence signals were simultaneously observed from CB[6]/DAH-HA hydrogel treated with both FITC-CB[6] and RBITC-CB[6] [(FITC-CB[6] + RBITC-CB[6])@CB[6]/DAH-HA hydrogel] (Figure 6b), demonstrating that several functional groups could be easily introduced at the same time to the supramolecular hydrogel in a modular manner using several different tags-CB[6]. The physical stability of CB[6]/DAH-HA hydrogel was not significantly affected by the treatment with tag-CB[6]. The G′ value of the $(HO)_{12}CB[6]$@CB[6]/DAH-HA hydrogel prepared by mixing CB[6]/DAH-HA hydrogel with 0.1 equiv of $(HO)_{12}CB[6]$[26] to the DAH moiety in the hydrogel was measured to be 2.2 ± 0.3 kPa (Figure S3b), which was comparable to that of the CB[6]/DAH-HA hydrogel (2.4 ± 0.2 kPa) (Figure 3b).
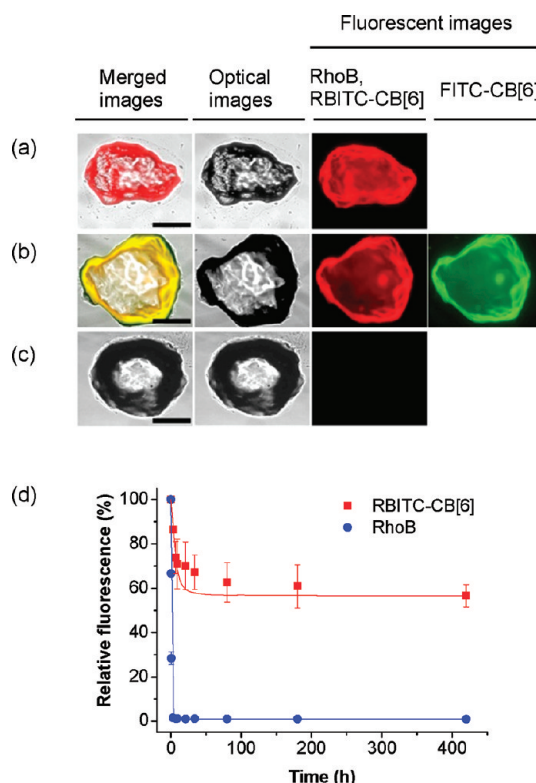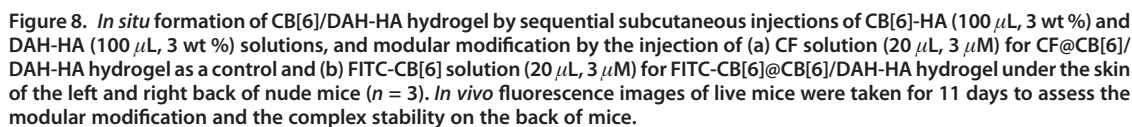

Figure 6. Modular modification of CB[6]/DAH-HA hydrogel with tags-CB[6] by highly selective host−guest interaction. CB[6]/DAH-HA hydrogels treated with (a) RBITC-CB[6], (b) RBITC-CB[6] + FITC-CB[6], and (c) RhoB (scale bar = 100 μm). (d) Relative fluorescence intensity (%) of RBITC-CB[6]@CB[6]/DAH-HA hydrogel and RhoB@CB[6]/DAH-HA hydrogel in PBS with increasing time (mean ± SD, n = 3).

Proliferation of Cells in c(RGDyK)-CB[6]@CB[6]/DAH-HA Hydrogels. To demonstrate the potential of CB[6]/DAH-HA hydrogels as a biocompatible artificial ECM for 3D cellular engineering, we decided to modify the 3D environment of CB[6]/DAH-HA hydrogel with a peptide of c(RGDyK) and investigate the behaviors of cells entrapped in the hydrogels. The c(RGDyK) is a fibronectin motif known to promote cell adhesion.[31] As described above, a simple treatment of CB[6]/DAH-HA hydrogel with c(RGDyK)-CB[6] (Figure 7c), synthesized in two steps from $(allyloxy)_{12}CB[6]$ (Figure S5), produced a c(RGDyK)-CB[6]@CB[6]/DAH-HA hydrogel. NHDF human fibroblast cells entrapped in the c(RGDyK)-CB[6]@CB[6]/DAH-HA hydrogel proliferated approximately 5-fold in 14 days (Figure 7a,d). In addition, NIH3T3 mouse fibroblast cells entrapped in c(RGDyK)-CB[6]@CB[6]/DAH-HA hydrogel for 3 days showed a spread morphology (Figure S6a). The results were thought to well match with the characteristic cell adhesion and proliferation behaviors under the RGD environment.[5,10] On the contrary, when the cells were incubated in CB[6]/DAH-HA hydrogels without the treatment of c(RGDyK)-CB[6], the cell proliferation within the hydrogel network was relatively low (Figure 7b,d) and the cells remained in a rounded

Figure 7. Confocal laser scanning microscopic images of NHDF cells entrapped in CB[6]/DAH-HA hydrogel (a) with or (b) without treatment of c(RGDyK)-CB[6] after cryosectioning and staining with DAPI. Magnified fluorescence images were taken in 14 days and overlapped with their respective bright-field images (scale bar = 50 μm). (c) Chemical structure of c(RGDyK)-CB[6]. (d) Number of DAPI-stained cells in 200 μm $\times$ 200 μm on the fluorescence images (mean $\pm$ SD, $n = 4$).

Figure 8. *In situ* formation of CB[6]/DAH-HA hydrogel by sequential subcutaneous injections of CB[6]-HA (100 μL, 3 wt %) and DAH-HA (100 μL, 3 wt %) solutions, and modular modification by the injection of (a) CF solution (20 μL, 3 μM) for CF@CB[6]/DAH-HA hydrogel as a control and (b) FITC-CB[6] solution (20 μL, 3 μM) for FITC-CB[6]@CB[6]/DAH-HA hydrogel under the skin of the left and right back of nude mice ($n = 3$). *In vivo* fluorescence images of live mice were taken for 11 days to assess the modular modification and the complex stability on the back of mice.

morphology with poor cell adhesion (Figure S6b). BrdU assay for cell proliferation also revealed that NIH3T3 cells cultured in c(RGDyK)-CB[6]@CB[6]/DAH-HA hydrogel proliferated much more actively (Figure S7b) than those cultured in CB[6]/DAH-HA hydrogel with (Figure S7c) and without free c(RGDyK) (Figure S7a). All of these results suggested that the c(RGDyK)-CB[6] treatment not only resulted in the capture of c(RGDyK) peptides in the CB[6]/DAH-HA hydrogels but also reconstituted a stable RGD environment for the efficient cellular adhesion and proliferation.

In Vivo Fluorescence Imaging of FITC-CB[6]@CB[6]/DAH-HA Hydrogels. Encouraged by the *in vitro* results, we further investigated whether the CB[6]/DAH-HA hydrogels could be exploited for *in vivo* applications. As shown in Figure 8, *in situ* formation of the hydrogel under the skin of nude mice was confirmed after sequential subcutaneous injections of CB[6]-HA solution and

PARK *ET AL.* VOL. 6 ▪ NO. 4 ▪ 2960–2968 ▪ 2012 ACSNANO 2965 www.acsnano.org

DAH-HA solution. The CB[6]/DAH-HA hydrogel was formed within a few minutes post-injection and stably kept its shape for longer than 2 weeks. In addition, we could demonstrate *in situ* modular modification of the hydrogel by simple injection of FITC-CB[6] into the hydrogel. The *in situ* modified hydrogel with FITC-CB[6] on the right back of the mouse emitted fluorescence for the next 11 days, whereas the hydrogel modified with carboxyfluorescein (CF) on the left back of the mouse as a control lost its fluorescence within a day probably due to the lack of strong interactions between the dye molecule and the hydrogel (Figure 8). Then, to evaluate the biocompatibility of CB[6]/DAH-HA hydrogels, histological analysis with hematoxylin and eosin (H&E) staining was performed in Balb/c mice after 1 week post-injection of the CB[6]/DAH-HA hydrogel precursor solutions. The CB[6]/DAH-HA hydrogels resulted in a negligible inflammation with comparable numbers of macrophages and lymphocytes to those of normal mice (Figure S8). The *in situ* facile formation and modular modification of the hydrogels on the back of mice reflected the feasibility of CB[6]/PA-HA hydrogels as a 3D biocompatible artificial ECM for *in vitro* studies on cellular behaviors, cell therapy, and various tissue engineering applications.

CONCLUSION

We successfully developed supramolecular HA hydrogels for 3D cellular engineering, taking advantage of the strong and selective host−guest interaction between CB[6] in CB[6]-HA and PA in PA-HA. The supramolecular assembly of CB[6]-HA and PA-HA in the presence of cells resulted in the *in situ* formation of cell-entrapped CB[6]/PA-HA hydrogels. Then, noncovalent, multifunctional, and modular modification of 3D environments of the hydrogels could be performed by the simple treatment with various tags-CB[6]. Furthermore, *in situ* formation of the CB[6]/PA-HA hydrogel was also demonstrated under the skin of nude mice by sequential subcutaneous injections of CB[6]-HA and DAH-HA solutions. The modularly modified hydrogel with FITC-CB[6] on the right back of nude mice emitted the fluorescence for up to 11 days, which suggested the feasibility of CB[6]/PA-HA hydrogels as a 3D biocompatible artificial ECM for various biomedical applications like *in vitro* studies on cellular behaviors, cell therapy, and tissue engineering.

MATERIALS AND METHODS

Materials. Sodium hyaluronate, sodium salt of hyaluronic acid (HA), with a molecular weight (MW) of 100 kDa was obtained from Shiseido (Tokyo, Japan), and HA with a MW of 234 kDa was purchased from Lifecore (Chaska, MN). Hyaluronidase from *Streptomyces hyalurolyticus*, phosphate buffered saline (PBS) tablet, *N*-hydroxysulfosuccinimide (sulfo-NHS), 1,6-diaminohexane (DAH), fluorescein isothiocyanate (FITC), and rhodamine B isothiocyanate (RBITC) were purchased from Sigma (St. Louis, MO). Spermine (SPM) and 1-ethyl-3-[3-(dimethylamino)propyl]carbodiimide (EDC) were obtained from Tokyo Chemical Industry (Tokyo, Japan). The aceto-methoxy derivative of calcein (Calcein AM), ethidium homo-dimer-1 (EthD-1), and 4′,6-diamidino-2-phenylindole (DAPI) were obtained from Molecular Probes (Carlsbad, CA). Cyclic RGDyK peptide [c(RGDyK)] was purchased from Peptron (Daejeon, Korea). SnakeSkin pleated dialysis tube was obtained from Thermo Scientific (Rockford, IL). Mouse embryonic fibroblast (NIH3T3) and normal human dermal fibroblast (NHDF) cell lines were obtained from American Type Culture Collection (ATCC). Dulbecco's modified Eagle's medium (DMEM), fetal bovine serum (FBS), and penicillin/streptomycin (PS) were obtained from HyClone (Logan, UT). Optimal cutting temperature (OCT) compounds (TISSUE-TEKs 4583) were purchased from Sakura Finetek (Torrance, CA), and Balb/c and nude mice were obtained from Clea in Japan. BrdU cell proliferation assay kit was obtained from Millipore (Billerica, MA). All reagents were used without further purification. Animal experiments were approved by the Animal Care Committee of CHA University.

Synthesis and Characterization of CB[6]-HA and PA-HA. CB[6]-conjugated HA (CB[6]-HA) was synthesized by thiol−ene "click" reaction[25] of thiol-functionalized HA (HS-HA, MW = 100 kDa)[26] with (allyloxy)$_{12}$CB[6] as we reported previously.[27,28] The photo-reactions were performed in a quartz tube by UV light using a RMR-600 (Rayonet, Branford, CT) photochemical reactor equipped with four 254 nm lamps and four 300 nm lamps. The resulting CB[6]-HA was analyzed by FT-IR (PerkinElmer, Waltham, MA) and ^{1}H NMR (DRX500, Bruker, Germany).[28] As a counterpart to CB[6]-HA for the hydrogel formation, two different alkylammonium-conjugated HAs, DAH-HA (MW = 270 kDa) and SPM-HA (MW = 320 kDa), were synthesized and characterized as reported elsewhere.[26,28] Briefly, 1 g of HA with a MW of 230 kDa was dissolved in 200 mL of distilled water. DAH or SPM (20 molar ratio of HA repeating unit) was added to the HA solution. Then, EDC and sulfo-NHS (4 molar ratio of HA) were added to activate the carboxyl groups of HA. The pH of the mixed solution was adjusted to 4.8 with 1 N HCl. After reaction in room temperature for 6 h, the resulting SPM-HA or DAH-HA conjugate was dialyzed against 100 mM sodium chloride solution for 3 days, 25% ethanol solution for a day, and distilled water for 12 h. The purified conjugate solution was lyophilized for 3 days. The degree of HA modification was analyzed by ^{1}H NMR (DRX-500, Bruker, Germany).

Preparation of CB[6]/DAH-HA Hydrogel or CB[6]/SPM-HA Hydrogel. A solution of DAH-HA or SPM-HA (300 μL, 2.0 wt %) in PBS was added to the equal volume of CB[6]-HA solution (2.0 wt %). Vortexing the solution for 10 s produced a CB[6]/PA-HA hydrogel.

Rheological Analysis. Rheological analysis was performed on a TA ARES rheometer with a parallel-plate geometry (20 mm diameter) at 25 °C. The initial hydrogel formation of the precursor solution (2.0 wt %) was observed by monitoring storage (G′) and loss (G″) moduli at a constant frequency of 100 rad/s with a fixed strain amplitude (10%) as a function of time. After complete gelation, the storage and loss moduli of a round shape molded CB[6]/DAH-HA hydrogel (1.0 cm in diameter and 0.3 mm in thickness) was monitored at a constant strain amplitude (10%) as a function of frequency to assess the mechanical property of the CB[6]/DAH-HA hydrogel.

Cell Viability Assessment. To analyze cell viability, a live/dead assay was performed with calcein AM and ethidium homodimer-1. The two components were added to PBS at a concentration of 2 and 4 μg/mL. The cell-entrapped hydrogels were then placed in the solution for 30 min and imaged under a fluorescence microscope. Live cells stain green, while dead cells uptake the red dye. The numbers of live and dead cells in 500 μm × 500 μm on the images were counted for the quantitative analysis (n = 4). In addition, the cell-entrapped CB[6]/DAH-HA

hydrogels were treated with and without hyaluronidase and observed under an optical microscope.

Modification of CB[6]/DAH-HA Hydrogel with RBITC-CB[6] and/or FITC-CB[6]. A solution of RBITC-CB[6] (50 μL, 60 μM) or RBITC-CB[6] (25 μL, 60 μM) + FITC-CB[6] (25 μL, 60 μM) was added to a CB[6]/DAH-HA hydrogel (600 μL, 2.0 wt %), which was kept in a humid chamber at room temperature for 2 h. The color of the whole hydrogel changed to the color of the RBITC-CB[6] solution. The hydrogel was then immersed in PBS (20 mL), and the PBS was exchanged every 8 h for a day to remove any unbound RBITC-CB[6]. A part of hydrogel, a few hundred micrometers in diameter, was extracted to confirm the successful modification of CB[6]/DAH-HA hydrogel with RBITC-CB[6] or RBITC-CB[6] + FITC-CB[6] under a fluorescence microscope with I3 filters (excitation 450−490 nm and emission >515 nm) for FITC and N2.1 filters (excitation 515−560 nm and emission >580 nm) for RBITC. As a control, the same experiment was performed with RhoB, the unconjugated fluorophore of RBITC instead of RBITC-CB[6]. The relative fluorescence intensity (%) (mean $\pm$ SD, $n = 3$) of RBITC-CB[6]@CB[6]/DAH-HA hydrogel and RhoB@CB[6]/DAH-HA hydrogel was monitored for 420 h.

Entrapment of Cells in c(RGDyK)-CB[6]@CB[6]/DAH-HA Hydrogel. NIH3T3 and NDHF cells were incubated in high-glucose DMEM containing 10% FBS and 1% PS at 37 °C and 5% CO_2. The cells were detached from culture substrates using trypsin, centrifuged with a centrifuge 5810R (Eppendorf) at 700 rpm for 5 min, and suspended in the solution of CB[6]-HA (2.0 wt %, 1×10^7 cells/mL). Each solution of DAH-HA (10.0 μL, 2.0 wt %) and c(RGDyK)-CB[6] (2.0 μL, 11.0 mM) was directly added to the solution of CB[6]-HA (10.0 μL, 2.0 wt %) containing NIH3T3 cells. The resulting solution was mixed to form a cell-entrapped hydrogel. The hydrogel was incubated in 2.0 mL of the culture medium at 5% CO_2 and 37 °C.

Cryosectioning of the Cell-Entrapped Hydrogels. NHDF cells (1×10^6 cells) were entrapped in c(RGDyK)-CB[6]@CB[6]/DAH-HA hydrogel (200 μL, 3 wt %) and CB[6]/DAH-HA hydrogel (200 μL, 3 wt %) and incubated in DMEM at 37 °C and 5% CO_2. The hydrogels entrapping cells were taken at 0 and 14 days and embedded in OCT compounds to be frozen. The frozen samples were cryosectioned at a thickness of 8 μm and mounted on glass slides. The sectioned samples were placed in paraformaldehyde (4%) solution containing DAPI (10 μg/mL) for 30 min and mounted in fluorescent mounting medium. The fluorescence from DAPI was observed with a confocal microscope (Nikon Eclipse TE 2000, Tokyo, Japan) at an excitation wavelength of 405 nm. The fluorescent cells in 200 μm $\times$ 200 μm on the images were counted for quantitative analysis ($n = 4$).

BrdU Assay for the Proliferation of Cells Entrapped in Hydrogels. NIH3T3 cells (2×10^4 cells) were entrapped in c(RGDyK)-CB[6]@CB[6]/DAH-HA hydrogel (100 μL, 2 wt %) and CB[6]/DAH-HA hydrogel (100 μL, 2 wt %) with and without c(RGDyK) (3 μL, 11 mM) in triplicate and incubated at 37 °C and 5% CO_2 in DMEM for 10 days. A solution of BrdU reagent (100 μL) was added to each well, and the plate was incubated at 37 °C in a tissue culture incubator for 3 h. After fixing the cells entrapped in the hydrogel, a solution of anti-BrdU monoclonal antibody was added to each well and the plate was incubated at room temperature for 1 h. The wells were washed and incubated with peroxidase-conjugated goat anti-mouse IgG at room temperature for 30 min. Then, the wells were incubated with TMB solution after washing at room temperature for 30 min in the dark. After mixing with a stop solution, the signal was detected at 450 nm using a microplate reader (EMax, Molecular Devices, CA).

***In Vivo* Fluorescence Imaging of FITC-CB[6]@CB[6]/DAH-HA Hydrogel.** CB[6]-HA (100 μL, 3 wt %) and DAH-HA (100 μL, 3 wt %) solutions were sequentially injected into the subcutis of the right and left side back of nude mice (6 week old, female, $n = 3$). After gentle touching the back of the mice for 30 s to produce CB[6]/DAH-HA hydrogels, FITC-CB[6] (20 μL, 3 μM) and CF (20 μL, 3 μM) solutions were injected into the hydrogel on the right and left back of the mice, respectively. At 0, 1, 4, 7, and 11 days post-injection, *in vivo* images of the fluorescence from the mice were obtained on a Xenogen IVIS system (Caliper Life Science).

Histological Analysis of CB[6]/DAH-HA Hydrogel. The biocompatibility of CB[6]/DAH-HA hydrogels was assessed in Balb/c mice

by the histological analysis after staining with hematoxylin and eosin (H&E). The CB[6]-HA solution (100 μL, 5 wt %) and the DAH-HA solution (100 μL, 5 wt %) were sequentially injected into the subcutis of the right back of Balb/c mice (6 week old female, $n = 3$). After 1 week post-injection, the implantation sites were completely excised and processed for the histological analysis. Biopsy samples were fixed in 4% formaldehyde solution, and fixed tissues were embedded in paraffin and sectioned at a thickness of 3 μm.

Statistical Analysis. The data are expressed as means $\pm$ standard deviation from several separate experiments. Statistical analysis was carried out *via* the two-way analysis of variance (ANOVA) test using the software of SigmaPlot10.0, and a value for *$P < 0.05$ was considered statistically significant.

Conflict of Interest: The authors declare no competing financial interest.

Supporting Information Available: Additional figures and a movie as discussed in the text. This material is available free of charge *via* the Internet at http://pubs.acs.org.

REFERENCES AND NOTES

1. Friedl, P.; Brocker, E. B. The Biology of Cell Locomotion within Three-Dimensional Extracellular Matrix. *Cell. Mol. Life Sci.* **2000**, *57*, 41–64.
2. Hoffman, A. S. Hydrogels for Biomedical Applications. *Adv. Drug Delivery Rev.* **2002**, *54*, 3–12.
3. Lutolf, M. P.; Hubbell, J. A. Synthetic Biomaterials as Instructive Extracellular Microenvironments for Morphogenesis in Tissue Engineering. *Nat. Biotechnol.* **2005**, *23*, 47–55.
4. Kiyonaka, S.; Sada, K.; Yoshimura, I.; Shinkai, S.; Kato, N.; Hamachi, I. Semi-Wet Peptide/Protein Array Using Supramolecular Hydrogel. *Nat. Mater.* **2004**, *3*, 58–64.
5. DeForest, C. A.; Polizzotti, B. D.; Anseth, K. S. Sequential Click Reactions for Synthesizing and Patterning Three-Dimensional Cell Microenvironments. *Nat. Mater.* **2009**, *8*, 659–664.
6. Ruel-Gariepy, E; Leroux, J. C. *In Situ*-Forming Hydrogels - Review of Temperature-Sensitive Systems. *Eur. J. Pharm. Biopharm.* **2004**, *58*, 409–426.
7. Chiu, Y. L.; Chen, S. C.; Su, C. J.; Hsiao, C. W.; Chen, Y. M.; Chen, H. L.; Sung, H. L. pH-Triggered Injectable Hydrogels Prepared from Aqueous *N*-Palmitoyl Chitosan: *In Vitro* Characteristics and *In Vivo* Biocompatibility. *Biomaterials* **2009**, *30*, 4877–4888.
8. Obara, K.; Ishihara, M.; Ishizuka, T.; Fujita, M.; Ozeki, Y.; Maehara, T.; Saitod, Y.; Yurad, H.; Matsuib, T.; Hattorib, H.; *et al.* Photocrosslinkable Chitosan Hydrogel Containing Fibroblast Growth Factor-2 Stimulates Wound Healing in Healing-Impaired db/db Mice. *Biomaterials* **2003**, *24*, 3437–3444.
9. Wu, D. Q.; Wang, T.; Lu, B.; Xu, X. D.; Cheng, S. X.; Jiang, X. J.; Zhang, X. Z.; Zhuo, R. X. Fabrication of Supramolecular Hydrogels for Drug Delivery and Stem Cell Encapsulation. *Langmuir* **2008**, *24*, 10306–10312.
10. Pek, Y. S.; Wan, A. C. A.; Shekaran, A.; Zhuo, L.; Ying, J. Y. A Thixotropic Nanocomposite Gel for Three-Dimensional Cell Culture. *Nat. Nanotechnol.* **2008**, *3*, 671–675.
11. Appel, E. A.; Biedermann, F.; Rauwald, U.; Jones, S. T.; Zayed, J. M.; Scherman, O. A. Supramolecular Cross-Linked Networks *via* Host−Guest Complexation with Cucurbit-[8]uril. *J. Am. Chem. Soc.* **2010**, *132*, 14251–14260.
12. Salem, A. K.; Rose, F. R. A. J.; Oreffo, R. O. C.; Yang, X. B.; Davies, M. C.; Mitchell, J. R.; Roberts, C. J.; Stolnik-Trenkic, S.; Tendler, S. J. B.; Williams, P. M.; *et al.* Porous Polymer and

Cell Composites That Self-Assemble *in Situ*. *Adv. Mater.* **2003**, *15*, 210–213.

13. Ehrbar, M.; Schoenmakers, R.; Christen, E. H.; Fussenegger, M.; Weber, W. Drug-Sensing Hydrogels for the Inducible Release of Biopharmaceuticals. *Nat. Mater.* **2008**, *7*, 800–804.

14. Kretschmann, O.; Choi, S. W.; Miyauchi, M.; Tomatsu, I.; Harada, A.; Ritter, H. Switchable Hydrogels Obtained by Supramolecular Cross-Linking of Adamantyl-Containing LCST Copolymers with Cyclodextrin Dimers. *Angew. Chem., Int. Ed.* **2006**, *45*, 4361–4365.

15. Okumura, Y.; Ito, K. The Polyrotaxane Gel: A Topological Gel by Figure-of-Eight Cross-Links. *Adv. Mater.* **2001**, *13*, 485–487.

16. Huh, K. M.; Ooya, T.; Lee, W. K.; Sasaki, S.; Kwon, I. C.; Jeong, S. Y.; Yui, N. Supramolecular-Structured Hydrogels Showing a Reversible Phase Transition by Inclusion Complexation between Poly(ethylene glycol) Grafted Dextran and α-Cyclodextrin. *Macromolecules* **2001**, *34*, 8657–8662.

17. Koopmans, C.; Ritter, H. Formation of Physical Hydrogels *via* Host−Guest Interactions of β-Cyclodextrin Polymers and Copolymers Bearing Adamantly Groups. *Macromolecules* **2008**, *41*, 7418–7422.

18. Mock, W. L. Cucurbituril. *Top. Curr. Chem.* **1995**, *175*, 1–24.

19. Kim, K. Mechanically Interlocked Molecules Incorporating Cucurbituril and Their Supramolecular Assemblies. *Chem. Soc. Rev.* **2002**, *31*, 96–107.

20. Kim, Y.; Kim, H.; Ko, Y. H.; Selvapalam, N.; Rekharsky, M. V.; Inoue, Y.; Kim, K. Complexation of Aliphatic Ammonium Ions with a Water-Soluble Cucurbit[6]uril Derivative in Pure Water: Isothermal Calorimetric, NMR, and X-ray Crystallographic Study. *Chem.—Eur. J.* **2009**, *15*, 6143–6151.

21. Park, K. M.; Suh, K.; Jung, H.; Lee, D. W.; Ahn, Y.; Kim, J.; Baek, K. K.; Kim, K. Cucurbituril-Based Nanoparticles: A New Efficient Vehicle for Targeted Intracellular Delivery of Hydrophobic Drugs. *Chem. Commun.* **2009**, *1*, 71–73.

22. Park, K. M.; Lee, D. W.; Sarkar, B.; Jung, H.; Kim, J.; Ko, Y. H.; Lee, K. E.; Jeon, H.; Kim, K. Reduction-Sensitive, Robust Vesicles with Noncovalently Modifiable Surface as a Multifunctional Drug Delivery Platform. *Small* **2010**, *6*, 1430–1441.

23. Kim, D.; Kim, E.; Kim, J.; Park, K. M.; Baek, K.; Jung, M.; Ko, Y. H.; Sung, W.; Kim, H. S.; Suh, J. H.; *et al.* Direct Synthesis of Polymer Nanocapsules with a Noncovalently Tailorable Surface. *Angew. Chem., Int. Ed.* **2007**, *46*, 3471–3474.

24. Lapcik, L., Jr.; Lapcik, L.; De Smedt, S.; Demeester, J.; Chabrecek, P. Hyaluronan: Preparation, Structure, Properties, and Applications. *Chem. Rev.* **1998**, *98*, 2663–2684.

25. Killops, K. L.; Campos, L. M.; Hawker, C. J. Robust, Efficient, and Orthogonal Synthesis of Dendrimers *via* Thiol-Ene "Click" Chemistry. *J. Am. Chem. Soc.* **2008**, *130*, 5062–5064.

26. Oh, E. J.; Park, K.; Kim, K. S.; Kim, J.; Yang, J. A.; Kong, J. H.; Lee, M. Y.; Hoffman, A. S.; Hahn, S. K. Target Specific and Long-Acting Delivery of Protein, Peptide, and Nucleotide Therapeutics Using Hyaluronic Acid Derivatives. *J. Controlled Release* **2010**, *141*, 2–12.

27. Kim, K.; Selvapalam, N.; Ko, Y. H.; Park, K. M.; Kim, D.; Kim, J. Functionalized Cucurbiturils and Their Applications. *Chem. Soc. Rev.* **2007**, *36*, 267–279.

28. Jung, H.; Park, K. M.; Yang, J. A.; Oh, E. J.; Lee, D. W.; Park, K. T.; Ryu, S. H.; Hahn, S. K.; Kim, K. Theranostic Systems Assembled *in Situ* on Demand by Host−Guest Chemistry. *Biomaterials* **2011**, *32*, 7687–7694.

29. Lutolf, M. P.; Lauer-Fields, J. L.; Schmoekel, H. G.; Metters, A. T.; Weber, F. E.; Fields, G. B.; Hubbell, J. A. Synthetic Matrix Metalloproteinase-Sensitive Hydrogels for the Conduction of Tissue Regeneration: Engineering Cell-Invasion Characteristics. *Proc. Natl. Acad. Sci. U.S.A.* **2003**, *100*, 5413–5418.

30. Csoka, A. B.; Frost, G. I.; Stern, R. The Six Hyaluronidase-like Genes in the Human and Mouse Genomes. *Matrix Biol.* **2001**, *20*, 499–508.

31. Pierschbacher, M. D.; Ruoslahti, E. Influence of Stereochemistry of the Sequence Arg-Gly-Asp-Xaa on Binding Specificity in Cell Adhesion. *J. Biol. Chem.* **1987**, *262*, 17294–17298.